SPOP mutations in prostate cancer across demographically diverse patient cohorts

Blattner, Mirjam ; Lee, Daniel J ; O'Reilly, Catherine ; Park, Kyung ; MacDonald, Theresa Y ; Khani, Francesca ; Turner, Kevin R ; Chiu, Ya-Lin ; Wild, Peter J ; Dolgalev, Igor ; Heguy, Adriana ; Sboner, Andrea ; Ramazangolu, Sinan ; Hieronymus, Haley ; Sawyers, Charles ; Tewari, Ashutosh K ; Moch, Holger ; Yoon, Ghil Suk ; Known, Yong Chul ; Andrén, Ove ; Fall, Katja ; Demichelis, Francecsa ; Mosquera, Juan Miguel ; Robinson, Brian D ; Barbieri, Christopher E ; Rubin, Mark A

Abstract: BACKGROUND: Recurrent mutations in the Speckle-Type POZ Protein (SPOP) gene occur in up to 15% of prostate cancers. However, the frequency and features of cancers with these mutations across different populations is unknown. OBJECTIVE: To investigate SPOP mutations across diverse cohorts and validate a series of assays employing high-resolution melting (HRM) analysis and Sanger sequencing for mutational analysis of formalin-fixed paraffin-embedded material. DESIGN SETTING AND PARTICIPANTS: 720 prostate cancer samples from six international cohorts spanning Caucasian, African American, and Asian patients, including both prostate-specific antigen-screened and unscreened populations, were screened for their SPOP mutation status. Status of SPOP was correlated to molecular features (ERG rearrangement, PTEN deletion, and CHD1 deletion) as well as clinical and pathologic features. RESULTS AND LIMITATIONS: Overall frequency of SPOP mutations was 8.1% (4.6% to 14.4%), SPOP mutation was inversely associated with ERG rearrangement (P<.01), and SPOP mutant (SPOPmut) cancers had higher rates of CHD1 deletions (P<.01). There were no significant differences in biochemical recurrence in SPOPmut cancers. Limitations of this study include missing mutational data due to sample quality and lack of power to identify a difference in clinical outcomes. CONCLUSION: SPOP is mutated in 4.6% to 14.4% of patients with prostate cancer across different ethnic and demographic backgrounds. There was no significant association between SPOP mutations with ethnicity, clinical, or pathologic parameters. Mutual exclusivity of SPOP mutation with ERG rearrangement as well as a high association with CHD1 deletion reinforces SPOP mutation as defining a distinct molecular subclass of prostate cancer.

DOI: https://doi.org/10.1593/neo.131704

Originally published at:
Blattner, Mirjam; Lee, Daniel J; O'Reilly, Catherine; Park, Kyung; MacDonald, Theresa Y; Khani, Francesca; Turner, Kevin R; Chiu, Ya-Lin; Wild, Peter J; Dolgalev, Igor; Heguy, Adriana; Sboner, Andrea; Ramazangolu, Sinan; Hieronymus, Haley; Sawyers, Charles; Tewari, Ashutosh K; Moch, Holger; Yoon, Ghil Suk; Known, Yong Chul; Andrén, Ove; Fall, Katja; Demichelis, Francecsa; Mosquera, Juan Miguel; Robinson, Brian D; Barbieri, Christopher E; Rubin, Mark A (2014). SPOP mutations in prostate cancer across demographically diverse patient cohorts. Neoplasia, 16(1):14-20.
DOI: https://doi.org/10.1593/neo.131704

NEOPLASIA
www.neoplasia.com
Volume 16 Number 1 January 2014 pp. 14–20 14

SPOP Mutations in Prostate Cancer across Demographically Diverse Patient Cohorts[1,2]

Mirjam Blattner*, Daniel J. Lee*,†, Catherine O'Reilly*, Kyung Park*, Theresa Y. MacDonald*, Francesca Khani*, Kevin R. Turner*, Ya-Lin Chiu‡, Peter J. Wild§, Igor Dolgalev¶, Adriana Heguy¶, Andrea Sboner*,#,, Sinan Ramazangolu*,#, Haley Hieronymus¶, Charles Sawyers¶, Ashutosh K. Tewari†, Holger Moch§, Ghil Suk Yoon††, Yong Chul Known‡‡, Ove Andrén§§,¶¶, Katja Fall##, Francecsa Demichelis**,***, Juan Miguel Mosquera*, Brian D. Robinson*,†, Christopher E. Barbieri*,†,3 and Mark A. Rubin*,†,**,3**

*Department of Pathology and Laboratory Medicine, Institute of Precision Medicine, Weill Medical College of Cornell University, New York, NY; †Department of Urology, Weill Medical College of Cornell University, New York, NY; ‡Department of Biostatistics and Epidemiology, Weill Medical College of Cornell University and New York-Presbyterian Hospital, New York, NY; §Institute of Surgical Pathology, University Hospital Zurich, Zurich, Switzerland; ¶Human Oncology and Pathogenesis Program, Memorial Sloan-Kettering Cancer Center, New York, NY; #Institute for Computational Biomedicine, Weill Medical College of Cornell University, New York, NY; **Institute for Precision Medicine, Weill Medical College of Cornell University, New York, NY; ††Department of Pathology, Kyungpook National University School of Medicine, Daegu, South Korea; ‡‡Department of Pathology, School of Medicine, Catholic University of Daegu, Daegu, South Korea; §§School of Health and Medical Sciences, Örebro University, Örebro, Sweden; ¶¶Department of Urology, Örebro University Hospital, Örebro, Sweden; ##Departments of Clinical Epidemiology and Biostatistics, School of Health and Medical Sciences, Örebro University, Örebro, Sweden; ***Centre for Integrative Biology, University of Trento, Trento, Italy

Abbreviations: AA, African American cohort from New York-Presbyterian Hospital; BCR, biochemical recurrence; FFPE, formalin fixation of tissue followed by paraffin embedding; HRM, high-resolution melting; MSKCC, Memorial Sloan-Kettering Cancer Center; PSA, prostate-specific antigen; SWWC, Swedish watchful waiting cohort; SPOPwt, SPOP wild type; SPOPmut, SPOP mutant; TURP, transurethral resection of the prostate; USZ, University Hospital of Zurich; WCMC, Weill Cornell Medical College

Address all correspondence to: Mark A. Rubin, MD, Department of Pathology and Laboratory Medicine, Weill Medical College of Cornell University, 1300 York Avenue, New York, NY 10065. E-mail: rubinma@med.cornell.edu

[1]This project was supported by the National Cancer Institute (1RO1CA125612 and 5UO1CA11275) as well as the Prostate Cancer Foundation. P.J.W. is supported by a SystemsX.ch grant (PhosphoNet-PPM). C.E.B. is supported by a Prostate Cancer Foundation Young Investigator Award and a Urology Care Foundation Research Scholar Award. A patent has been issued to Weill Medical College of Cornell University on *SPOP* mutations in prostate cancer; C.E.B. and M.A.R. are listed as co-inventors.
[2]This article refers to supplementary materials, which are designated by Table W1 and Figure W1 and are available online at www.neoplasia.com.
[3]These authors shared senior authorship.
Received 27 September 2013; Revised 17 December 2013; Accepted 19 December 2013

DOI 10.1593/neo.131704

Abstract

BACKGROUND: Recurrent mutations in the Speckle-Type POZ Protein (*SPOP*) gene occur in up to 15% of prostate cancers. However, the frequency and features of cancers with these mutations across different populations is unknown. *OBJECTIVE:* To investigate *SPOP* mutations across diverse cohorts and validate a series of assays employing high-resolution melting (HRM) analysis and Sanger sequencing for mutational analysis of formalin-fixed paraffin-embedded material. *DESIGN, SETTING, AND PARTICIPANTS:* 720 prostate cancer samples from six international cohorts spanning Caucasian, African American, and Asian patients, including both prostate-specific antigen–screened and unscreened populations, were screened for their *SPOP* mutation status. Status of *SPOP* was correlated to molecular features (*ERG* rearrangement, *PTEN* deletion, and *CHD1* deletion) as well as clinical and pathologic features. *RESULTS AND LIMITATIONS:* Overall frequency of *SPOP* mutations was 8.1% (4.6% to 14.4%), *SPOP* mutation was inversely associated with *ERG* rearrangement ($P < .01$), and *SPOP* mutant (*SPOPmut*) cancers had higher rates of *CHD1* deletions ($P < .01$). There were no significant differences in biochemical recurrence in *SPOPmut* cancers. Limitations of this study include missing mutational data due to sample quality and lack of power to identify a difference in clinical outcomes. *CONCLUSION: SPOP* is mutated in 4.6% to 14.4% of patients with prostate cancer across different ethnic and demographic backgrounds. There was no significant association between *SPOP* mutations with ethnicity, clinical, or pathologic parameters. Mutual exclusivity of *SPOP* mutation with *ERG* rearrangement as well as a high association with *CHD1* deletion reinforces *SPOP* mutation as defining a distinct molecular subclass of prostate cancer.

Neoplasia (2014) 16, 14–20

Introduction

Prostate cancer is a significant health burden, with 241,740 new diagnoses and 28,170 deaths in the United States in 2012 [1]. The inability to distinguish indolent from aggressive disease is a challenge [2]. Identification of driver lesions for specific subsets of prostate cancer could ultimately lead to the development of biomarkers to improve prognostic ability and risk stratification.

Recent advances have uncovered multiple recurrent alterations in prostate cancer. The *TMPRSS2-ERG* fusion has been observed in nearly 50% of prostate cancers [3,4].

We recently reported somatic mutations in the Speckle-Type POZ Protein (*SPOP*) gene in 6% to 15% of prostate cancers [5]. *SPOP* mutations define a distinct subclass of prostate cancer: *SPOP* mutations and *ETS* rearrangements are mutually exclusive; *SPOP* mutant (*SPOPmut*) prostate tumors generally lack lesions in the phosphatidylinositide 3-kinase (PI3K) pathway, and they are also independent of mutations in the tumor suppressor gene *TP53* [5–7].

Although the recurrent nature of *SPOP* mutations is clear, less is known about the frequency of *SPOP* mutations across different ethnicities and screening practices, the associations with clinical and pathologic characteristics, and the effects on patient outcomes. This study represents the largest multi-institutional study to date investigating these associations with *SPOP* mutations across different cohorts.

In addition, detection of *SPOP* mutations in older well-annotated archival prostate cancer samples represents a technical challenge. Formalin fixation of tissue followed by paraffin embedding (FFPE) is widely used; however, analysis of nucleic acid from FFPE material is difficult due to cross-linking between nucleic acid and proteins [8]. The tissue heterogeneity in prostate cancer samples can dilute the signal of tumor-associated mutations with benign wild-type contamination and make the detection of point mutations difficult.

In an effort to overcome these challenges, we developed a series of assays employing high-resolution melting (HRM) analysis, which relies on alterations in the melting curve of mutated nucleic acids, and Sanger sequencing [9–11]. We optimized the HRM assay as a high sensitivity pre-screening tool, followed by Sanger sequencing for specific confirmation of mutations. Finally, we employed a next-generation sequencing approach on a small subset of samples to determine if massively parallel sequencing could rescue samples considered assay failures using the HRM-Sanger methods.

Materials and Methods

Patient Populations

Table 1 lists the clinical, pathologic, and survival data according to each cohort. In total, prostate cancer samples from 996 patients [radical prostatectomy (RP), transurethral resection of the prostate (TURP), or metastatic biopsies] were examined. Of the 996 patients, 720 samples had DNA of sufficient quality and were screened for their *SPOP* status. Cohorts included patients from Memorial Sloan-Kettering Cancer Center (MSKCC), cohort from Kyungpook National University School of Medicine, Korea (Korean), African American cohort from New York-Presbyterian Hospital (AA), Weill Cornell Medical College (WCMC) cohorts, and University Hospital of Zurich (USZ), as well as the Swedish watchful waiting cohort (SWWC). A detailed description about each individual cohort can be found in the Supplementary Materials and Methods. Samples were categorized into *SPOP* wild type (*SPOPwt*) and *SPOPmut* and analyzed for correlation

Table 1. Demographics by Cohort.

	N	Median Age	Median PSA	Pathologic Gleason Grade			Pathologic Stage			Clinical Outcomes		
				6	7	8 to 10	pT2	pT3	pT4	PSM	+BCR	DOD
African American	105	61	5.6	19 (18.1%)	79 (75.2%)	5 (6.7%)	85 (81.0%)	20 (19.0%)		13 (12.4%)	12 (11.4%)	NA
Korean	127	67	10.4	14 (12.6%)	70 (63.1%)	27 (24.3%)	45 (35.4%)	82 (64.6%)		66 (52%)	22 (17.6%)	NA
Swedish	141	74	NA	25 (17.7%)	61 (43.3%)	55 (39.0%)	NA	NA	NA	NA	NA	93 (66%)
Zurich	421	66	11	54 (14.8%)	186 (51.0%)	125 (34.3%)	181 (60.5%)	106 (35.5%)	12 (4.0%)	NA	62 (32.8%)	24 (9.1%)
MSKCC	218	58.2	6.6	51 (26.7)	107 (56.0%)	33 (17.3)	109 (56.2%)	65 (33.5%)	20 (10.3)	53 (26.5)	39 (30.7)	4 (1.9%)
WCMC	125	63	5.0	12 (9.7%)	93 (75.0%)	19 (15.3%)	62 (69.7%)	27 (30.3%)		15 (20.0%)	11 (15.3%)	NA

PSM indicates positive surgical margin; +BCR, positive biochemical recurrence; DOD, died of disease.

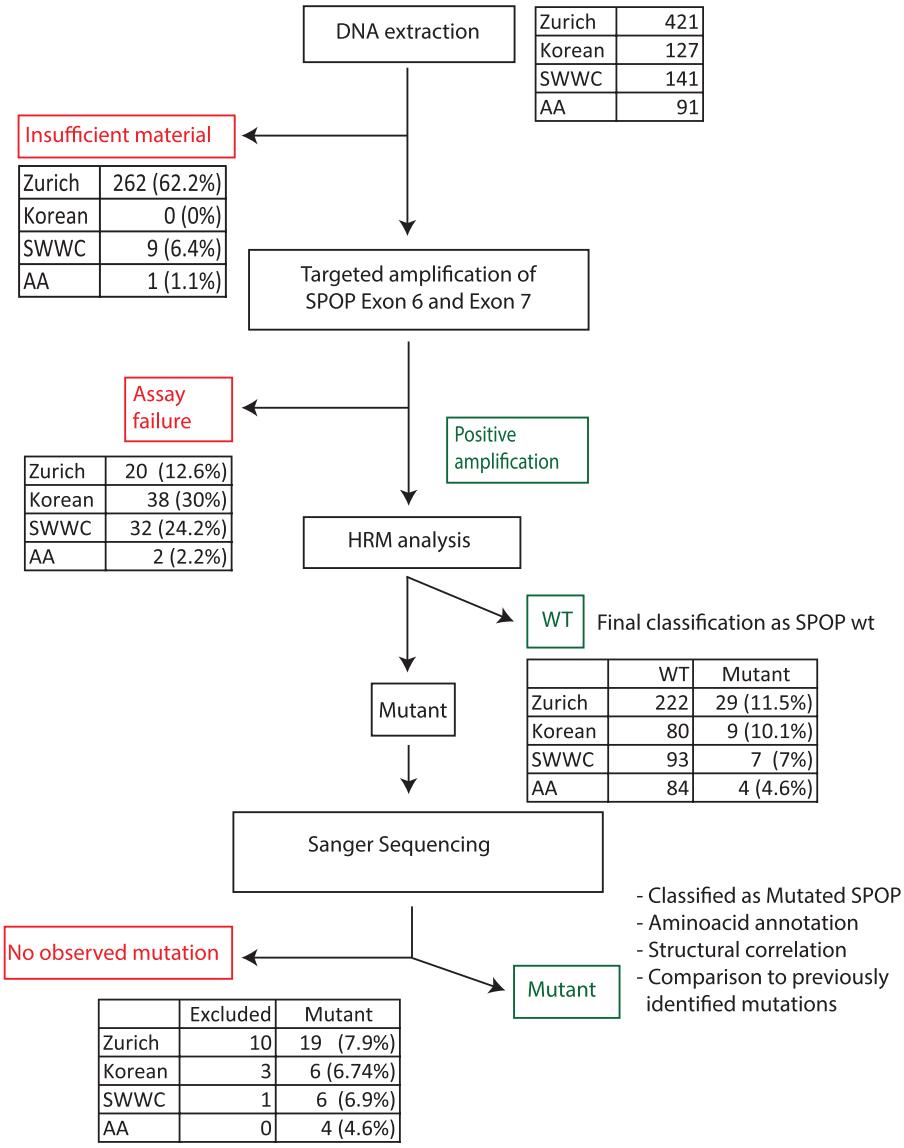

Figure 1. Workflow of specimen screening process. The workflow of the sample screening process for 421, 127, 141, and 61 samples from the Zurich, Korean, SWWC, and AA cohorts is shown. A number of at least three 0.6-mm cores were obtained for DNA extraction. The DNA concentrations of 226 (Zurich), 9 (SWWC), and 1 (AA) samples were less than 20 to 50 ng/μl and therefore excluded from the study. Of the remaining samples, 20 (Zurich), 38 (Korean), 32 (SWWC), and 2 (AA) failed the PCR-based assay. By the HRM assay, 222 (Zurich), 80 (Korean), 93 (SWWC), and 84 (AA) samples were classified as *SPOPwt*. Twenty-nine (Zurich), 9 (Korean), 7 (SWWC), and 4 (AA) samples that had a melting curve shift were sent off for Sanger sequencing for further characterization. A mutation in either exon 6 or exon 7 of the *SPOP* gene was found in 19 (Zurich), 6 (Korean), 6 (SWWC), and 4 (AA) samples. No alteration was found for the remaining 10 (Zurich), 3 (Korean), and 1 (SWWC) samples and therefore excluded from the study. Numbers shown in the tables indicate the number of samples per processing step and their percentage.

between *SPOP* mutation and pathologic-clinical data. Pathologists with expertise in genitourinary pathology reviewed the archival material at each participating institution. Institutional Review Board approval was obtained at all participating sites.

Patient-Related Variables

All clinical and pathologic data were prospectively collected by each individual center, including information on patient age, preoperative prostate-specific antigen (PSA) level, Gleason score, pathologic stage, surgical margin status, and biochemical recurrence (BCR). Detailed description of staging and BCR as well as PSA characterization can be found in the Supplementary Materials and Methods. For a subset of 118 unselected prostate cancers from the WCMC cohort, 15 morphologic features of prostate cancer were assessed (Qiagen, Hilden, Germany). A detailed description of the morphologic features as well as the process of review is described in the Supplementary Materials and Methods.

DNA Extraction

DNA for the AA and Korean cohorts and SWWC was extracted from tissue cores using a Qiagen BioRobot Universal System. Detailed description of the protocol can be found in the Supplementary Materials and Methods. Detailed description of DNA extraction for the cohorts from WCMC, MSKCC, as well as Zurich have been previously described [5,12,13].

Targeted Enrichment for SPOP *Exons 6 and 7 and HRM Analysis*

The mutational screening assay involves an initial pre–polymerase chain reaction (PCR) amplification step to enrich the target region followed by an HRM screen and Sanger sequencing. PCR assay setup, as well as cycling conditions, HRM assay, and analysis are described in the Supplementary Materials and Methods.

Sanger Sequencing

PCR products were purified using Qiagen PCR purification kit and eluted as per the manufacturers' instructions and sent for Sanger sequencing a minimum of three times to confirm the mutation status. (For a complete list of primers, see Table W1.)

Fluorescence In Situ *Hybridization and Immunohistochemistry*

Fluorescence *In Situ* Hybridization (FISH) methods to detect *TMPRSS2-ETS* gene fusions have been previously described [3,14]. We used *ERG* break-apart FISH assays to confirm gene rearrangement on the DNA level [15]. To assess the status of *PTEN*, we used a locus-specific probe and a reference probe, as previously described [16], and a similar approach was used to detect CHD1 deletions. The sequences of all FISH probes are listed in Table W1. *ERG* expression was assessed by immunohistochemistry, as previously described [17].

DNA Capture, Library Preparations, and MiSeq Runs

A customized TrueSeq amplicon kit was designed by using Illumina DesignStudio, and the library preparation was performed as suggested by the manufacturer. More information about the design and the library preparation can be found in the Supplementary Materials and Methods.

Alignment and Analysis

Reads were aligned independently to the human genome reference sequence (GRC37/hg19) using a Smith-Waterman mode BWA [18] to maximize the number of reads aligned to the genome. An in-house tool was then used to determine the genotype of the locations of *SPOP*.

Statistical Analysis

Results were expressed as a contingency table to show association between *SPOP* status with clinical and pathologic variables along with available molecular data (Table 3). Differences were considered statistically significant at $P < .05$. All statistical analyses were performed with Stata SE, version 11.0 (StataCorp, College Station, TX).

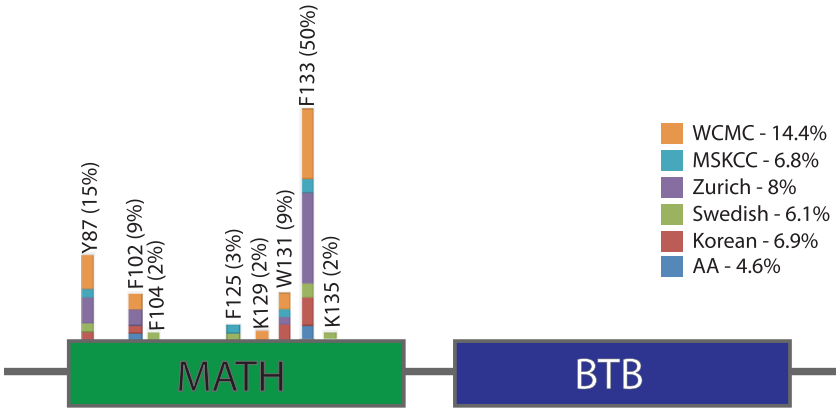

Figure 2. Schematic overview of the *SPOP* gene and localization of mutations. The two protein domains, meprin and TRAF homology (MATH) and broad complex, tramtrack and bric-a-brac (BTB), and the specific amino acid positions harboring the alterations and its relative recurrence are shown. The proportion of the colors in bars indicates the abundance of the mutation in each of the six cohorts, WCMC (orange), MSKCC (light blue), Zurich (purple), Swedish (green), Korean (red), and AA (dark blue). The overall frequency of mutated SPOP in the cohort is shown next to the color coding system.

Table 2. Molecular Alterations by Cohort.

	No. of Evaluable Samples	SPOP		ERG		PTEN		CHD1	
		Wild Type	Mutant	Wild Type	Positive	Wild Type	Deletion	Wild Type	Deletion
African American	88	84 (95.4%)	4 (4.6%)	66 (75.0%)	22 (25.0%)	78 (91.8%)	7 (8.2%)	NA	NA
Korean	87	81 (93.1%)	6 (6.9%)	55 (70.5%)	23 (29.5%)	53 (82.8%)	11 (17.2%)	NA	NA
Swedish	99	93 (93.9%)	6 (6.1%)	79 (79.8%)	20 (20.2%)	NA	NA	52 (82.5%)	11 (17.5%)
Zurich	241	222 (92.1%)	19 (7.9%)	80 (45.5%)	96 (54.5%)	93 (51.7%)	87 (48.3%)	NA	NA
MSKCC	80	75 (93.7%)	5 (6.3%)	38 (47.5%)	42 (52.5%)	75 (93.8%)	5 (6.3%)	67 (87.0%)	10 (13.0%)
WCMC	125	107 (85.6%)	18 (14.4%)	65 (61.9%)	37 (35.2%)	82 (81.2%)	19 (18.8%)	36 (70.6%)	15 (29.4%)

Results

Performance of HRM Assay

In this study, we screened 996 samples from six independent cohorts: WCMC, AA, Korean, MSKCC, Zurich, and SWWC for their *SPOP* status. Of 996 samples, we were able to successfully evaluate *SPOP* status in 720 samples (72.3%), which were classified into 662 *SPOPwt* and 58 *SPOPmut* samples. A flowchart of sample testing is shown in Figure 1. To determine the sensitivity of HRM and reliability for annotating wild-type samples, 100 samples with wild-type HRM results (no shift) were subsequently Sanger sequenced. All 100 samples were *SPOPwt*. A dilution series of plasmid DNA showed that less than 5% of *SPOPmut* DNA was sufficient for a notable shift in the melting curve (Figure W1).

A subset of 22 samples was flagged positive by HRM but could not be validated by Sanger sequencing due to assay failure; deep sequencing of those samples was attempted on the MiSeq platform; however, overall read quality was poor and we therefore excluded those samples from the study. With an overall coverage of 98.7% of the *SPOP* exome and an average number of 591,242 mapped reads for 10 control samples, 6 FFPE material and 4 fresh frozen, the efficiency of the capture assay and the sequencing was demonstrated.

Table 3. Demographics and Molecular Changes by SPOP Mutation.

	WT	+SPOP	*P* Value
N (%)	662/720 (91.9%)	58/720 (8.1%)	
Median age	65 (34-89)	64 (46-84)	0.49
Median PSA	7.1	7.4	0.65
Gleason grade			0.26
6	97 (15.9%)	4 (7.3%)	
3 + 4	230 (37.7%)	20 (36.4%)	
4 + 3	132 (21.6%)	16 (29.1%)	
8 to 10	151 (24.8%)	15 (27.3%)	
Pathologic stage			0.58
pT2	298 (62.6%)	29 (70.7%)	
pT3	166 (34.9%)	12 (29.3%)	
pT4	12 (2.5%)	0	
Median follow-up time, months (range)	73 (1.9-182)	100.5 (13-160)	0.67
Positive BCR	70 (19.9%)	7 (25.9%)	0.45
Median time to BCR, months (range)	18 (1.2-139)	15 (11-55.4)	0.29
Status			0.69
NED	158 (50.8%)	10 (47.6%)	
AWD	65 (20.9%)	6 (28.6%)	
DOD	77 (24.8%)	4 (19.0%)	
DOC	11 (3.5%)	1 (4.8%)	
ERG			<0.01
WT	337 (59.4%)	46 (95.8%)	
Positive	230 (40.6%)	2 (4.2%)	
PTEN			0.31
WT	350 (74.1%)	31 (81.6%)	
Deletion	122 (25.9%)	7 (18.4%)	
CHD1			<0.01
WT	147 (85.0%)	8 (42.1%)	
Deletion	26 (15.0%)	11 (57.9%)	

BCR indicates biochemical recurrence; AWD, alive with disease; NED, no evidence of disease; DOD, died of disease; DOC, died of other causes; WT, wild type.

SPOP *Mutation across Cohorts*

SPOP mutations were detected in 58/720 evaluable cases (8.1%) targeting all previously detected mutations in prostate cancer. Consistent with previous results, the most frequently mutated residue was F133 (50%) followed by Y87 (15%), W131 and F102 (9%), F125 (3%), and K129, F104, and K135 (2%). All mutations were missense and clustered in the substrate binding MATH domain (Figure 2). Mutations at F104 and K135 have not been previously described.

Association of SPOP *Mutation with Clinicopathologic Characteristics and Outcomes*

The clinicopathologic characteristics of the 996 patients are summarized in Table 1. Overall, the rate of *SPOP* mutation was 8.1% (4.6%-14.4%, see Table 2). The AA cohort had the lowest rate of *SPOP* mutations (4.6%), and the highest rate was in the WCMC cohort (14.4%), but there were no significant differences between cohorts ($P = .14$). Patients with *SPOP* mutations had no significant differences in Gleason grade and rates of BCR ($P = .26$ and $P = .18$, respectively; Table 3). In a separate sub-analysis, those who had treatment for their prostate cancer by RP ($N = 911$) were compared to those who received only palliative treatment (i.e., TURP; $N = 197$), and no significant differences were noted in frequency of SPOP mutations (8.75 *vs* 6.1%, $P = .40$). Patients with mutant *SPOP* had a median time to BCR of 15 months compared to 18 months for *SPOPwt* ($P = .30$). There were no significant differences noted in age, preoperative PSA, lymph node positivity, or pathologic stage according to *SPOP* mutation status. There were also no noted differences in survival according to *SPOP* status ($P = .78$). There were no significant associations noted with *SPOP* mutations on univariable or multivariable Cox regression models for relapse-free survival, cancer-specific survival, and overall survival ($P = .57, .62, .75$, respectively).

Association of SPOP *Mutations with Morphologic Features of Prostate Cancer*

No morphologic features were associated with positive *SPOPmut* status. Cribriform morphology was present in 64% of *SPOPmut* compared to 18% in nonmutants ($P = .08$). Foamy gland morphology showed a significant negative association with *SPOPmut*, with 18% of *SPOPmut* cases exhibiting this feature compared to 72% of control cases ($P = .03$). However, when this *P* value was adjusted to account for multiple comparisons (Bonferroni method), the statistical significance was lost.

Association of SPOP *Mutations with Other Molecular Alterations*

Across all six cohorts, the frequency of *ERG* rearrangement was 38.3% (range, 20.2%-54.5%), *PTEN* deletions 25.3% (6.3%-48.3%), and *CHD1* deletions 19.3% (13.0%-29.4%). We found only two *SPOPmut* cases with an *ERG* rearrangement ($P < .01$), consistent with previously reported mutual exclusivity [5]. There were no significant associations between *SPOP* mutations and *PTEN* deletions ($P = .31$) despite previously reported inverse association in clinically localized disease [5]. Patients with *SPOP* mutations demonstrated significantly higher rates of *CHD1* deletion (57.9% *vs* 15.0%, respectively, $P < .01$).

Discussion

This study represents the largest multi-institutional collaboration to evaluate for *SPOP* mutations across different populations. In the current study, the rate of *SPOP* mutations was similar across different ethnicities and cohorts, at a rate of 8.1% of prostate cancers, ranging from 4.6% in the AA cohort to 14% in the WCMC cohort. In addition, differences in *SPOP* frequency might be influenced by intratumor heterogeneity, prostate tumor density, tumor multifocality and sample handling variations among different institutions. Method of detection and sample quality may also play a role; next-generation sequencing and high-quality tissue specimens will likely maximize sensitivity. Finally, subclonality of certain point mutations will likely impact detection rates. SPOP mutations have been shown to be highly clonal [19], limiting this concern for these specific mutations, but the heterozygous nature of SPOP mutations does impact sensitivity.

Previous studies have suggested that *SPOP* mutations identify a distinct molecular subclass of prostate cancer compared to ETS family rearrangements [5,20]. This study confirms those findings; of 58 *SPOP*-mutated cases, only two showed an *ERG* rearrangement in the same patient. Co-occurrence of *SPOP* mutation and *ERG* rearrangement may be due to sampling adjacent but molecularly distinct tumor foci in the same specimen, as previously described [5], or as a result of intratumoral heterogeneity. We also cannot exclude the possibility that *SPOP* mutations and *ETS* rearrangement do occur together in the same tumor cells at exceptionally low frequency.

SPOP mutations are also associated with *CHD1* deletions [5,19]. In this study, 57.9% of the *SPOPmut* harbored *CHD1* deletions. These findings suggest that *SPOP* mutations may be driver lesions in a distinct molecular subclass of prostate cancer. Across all cohorts, we saw no significant association between *PTEN* deletion and *SPOP* mutation. We had previously reported an inverse association between *SPOP* mutation and *PTEN* lesions in clinically localized prostate cancer but in a PSA-screened population of primarily Caucasian men [5]. Previously, we observed no association between *SPOP* mutation and *PTEN* deletions in metastatic cancer, highlighting that the relationship between these two abnormalities is highly dependent on the context of the specific patient cohort.

We detected no signification difference in rates or time to BCR in relation to SPOP status. However, despite the considerable sample size, the study was underpowered to evaluate oncologic outcomes in relation to *SPOP* status: Assuming a 15% rate of BCR rate after 5 years of definitive surgical management according to recent large studies [21–23], and assuming an overall *SPOP* mutation rate of approximately 10% [5], to achieve at least 80% power to detect a significant difference in BCR, the sample size would need to be several thousand patients with long-term follow-up. With the establishment of assays defined here, we can continue multi-institutional collaborative efforts to identify associations of *SPOP* mutation with clinical outcomes to connect molecular classification with risk stratification.

We have developed an HRM-based screening assay, which allows us to screen samples from archival FFPE material in a high-throughput and cost-efficient manner. This assay demonstrates high sensitivity, reliability, and efficiency. Less than 5% mutated tumor DNA has to be present to lead to a positive result. However, it is important to note that no mutation calls were made solely based on HRM; all potential mutations were verified by Sanger sequencing. Sanger sequencing has a sensitivity of roughly 20% [24], making the HRM assay considerably more sensitive but difficult to validate. Samples showing a shift on HRM but no mutation by sequencing were classified as assay failures and excluded to rule out false-negative calls. One concern about archival material is the potential poor quality of the DNA. Most likely poor DNA quality was the reason for the assay failure rate (28.3% of all samples). Assay failure could not be rescued by next-generation sequencing, reinforcing that the sample characteristics were likely more important than the assay characteristics.

Our study is the first to examine morphologic features of *SPOPmut* prostate cancer. Although the clinical significance of *SPOPmut* status is yet to be established, we sought to assess if *SPOPmut* prostate cancer could be recognized histologically. When subsets of *SPOPmut* and *SPOPwt* cases with similar Gleason score and pathologic stage were compared, no morphologic features were associated with positive *SPOPmut* status.

In conclusion, we have shown that *SPOP* is mutated in 4.6% to 14.4% of prostate cancers in six cohorts with different ethnic and demographic backgrounds. There was no significant difference in *SPOP* mutation frequency among cohorts. Mutual exclusivity of mutated *SPOP* and *ERG* rearrangement as well as high correlation of *SPOP* mutation with deletion of *CHD1* across different cohorts and ethnicities reinforces *SPOP* mutation as defining a distinct subclass of prostate cancer. Further studies, potentially with large numbers of patients, will be needed to determine the impact of *SPOP* mutation on clinical outcome.

Acknowledgments

We are grateful to patients and families who contributed to this study, their doctors, and all the contributing centers, which made it possible. We thank R. Kim and R. Leung for their critical contributions to the Weill Cornell Prostate Cancer Tumor Bank, S. Dettwiler for assistance with the USZ cohort, and A. Romanel for his contribution to the computational analysis of the sequencing data.

References

[1] Siegel R, Naishadham D, and Jemal A (2012). Cancer statistics, 2012. *CA Cancer J Clin* **62**, 10–29.

[2] Sartor AO, Hricak H, Wheeler TM, Coleman J, Penson DF, Carroll PR, Rubin MA, and Scardino PT (2008). Evaluating localized prostate cancer and identifying candidates for focal therapy. *Urology* **72**, S12–S24.

[3] Tomlins SA, Rhodes DR, Perner S, Dhanasekaran SM, Mehra R, Sun XW, Varambally S, Cao X, Tchinda J, Kuefer R, et al. (2005). Recurrent fusion of *TMPRSS2* and ETS transcription factor genes in prostate cancer. *Science* **310**, 644–648.

[4] Perner S, Demichelis F, Beroukhim R, Schmidt FH, Mosquera JM, Setlur S, Tchinda J, Tomlins SA, Hofer MD, Pienta KG, et al. (2006). *TMPRSS2:ERG* fusion-associated deletions provide insight into the heterogeneity of prostate cancer. *Cancer Res* **66**, 8337–8341.

[5] Barbieri CE, Baca SC, Lawrence MS, Demichelis F, Blattner M, Theurillat JP, White TA, Stojanov P, Van Allen E, Stransky N, et al. (2012). Exome sequencing

identifies recurrent SPOP, FOXA1 and MED12 mutations in prostate cancer. *Nat Genet* **44**, 685–689.

[6] Zhuang M, Calabrese MF, Liu J, Waddell MB, Nourse A, Hammel M, Miller DJ, Walden H, Duda DM, Seyedin SN, et al. (2009). Structures of SPOP-substrate complexes: insights into molecular architectures of BTB-Cul3 ubiquitin ligases. *Mol Cell* **36**, 39–50.

[7] Lindberg J, Klevebring D, Liu W, Neiman M, Xu J, Wiklund P, Wiklund F, Mills IG, Egevad L, and Gronberg H (2013). Exome sequencing of prostate cancer supports the hypothesis of independent tumour origins. *Eur Urol* **63**, 347–353.

[8] Solassol J, Ramos J, Crapez E, Saifi M, Mange A, Vianes E, Lamy PJ, Costes V, and Maudelonde T (2011). KRAS mutation detection in paired frozen and formalin-fixed paraffin-embedded (FFPE) colorectal cancer tissues. *Int J Mol Sci* **12**, 3191–3204.

[9] Wittwer CT, Reed GH, Gundry CN, Vandersteen JG, and Pryor RJ (2003). High-resolution genotyping by amplicon melting analysis using LCGreen. *Clin Chem* **49**, 853–860.

[10] Ririe KM, Rasmussen RP, and Wittwer CT (1997). Product differentiation by analysis of DNA melting curves during the polymerase chain reaction. *Anal Biochem* **245**, 154–160.

[11] Reed GH, Kent JO, and Wittwer CT (2007). High-resolution DNA melting analysis for simple and efficient molecular diagnostics. *Pharmacogenomics* **8**, 597–608.

[12] Mortezavi A, Hermanns T, Seifert HH, Baumgartner MK, Provenzano M, Sulser T, Burger M, Montani M, Ikenberg K, Hofstadter F, et al. (2011). KPNA2 expression is an independent adverse predictor of biochemical recurrence after radical prostatectomy. *Clin Cancer Res* **17**, 1111–1121.

[13] Taylor BS, Schultz N, Hieronymus H, Gopalan A, Xiao Y, Carver BS, Arora VK, Kaushik P, Cerami E, Reva B, et al. (2010). Integrative genomic profiling of human prostate cancer. *Cancer Cell* **18**, 11–22.

[14] Tomlins SA, Laxman B, Dhanasekaran SM, Helgeson BE, Cao X, Morris DS, Menon A, Jing X, Cao Q, Han B, et al. (2007). Distinct classes of chromosomal rearrangements create oncogenic ETS gene fusions in prostate cancer. *Nature* **448**, 595–599.

[15] Svensson MA, LaFargue CJ, MacDonald TY, Pflueger D, Kitabayashi N, Santa-Cruz AM, Garsha KE, Sathyanarayana UG, Riley JP, Yun CS, et al. (2011). Testing mutual exclusivity of ETS rearranged prostate cancer. *Lab Invest* **91**, 404–412.

[16] Berger MF, Lawrence MS, Demichelis F, Drier Y, Cibulskis K, Sivachenko AY, Sboner A, Esgueva R, Pflueger D, Sougnez C, et al. (2011). The genomic complexity of primary human prostate cancer. *Nature* **470**, 214–220.

[17] Park K, Tomlins SA, Mudaliar KM, Chiu YL, Esgueva R, Mehra R, Suleman K, Varambally S, Brenner JC, MacDonald T, et al. (2010). Antibody-based detection of *ERG* rearrangement–positive prostate cancer. *Neoplasia* **12**, 590–598.

[18] Li H and Durbin R (2010). Fast and accurate long-read alignment with Burrows-Wheeler transform. *Bioinformatics* **26**, 589–595.

[19] Baca SC, Prandi D, Lawrence MS, Mosquera JM, Romanel A, Drier Y, Park K, Kitabayashi N, MacDonald TY, Ghandi M, et al. (2013). Punctuated evolution of prostate cancer genomes. *Cell* **153**, 666–677.

[20] Grasso CS, Wu YM, Robinson DR, Cao X, Dhanasekaran SM, Khan AP, Quist MJ, Jing X, Lonigro RJ, Brenner JC, et al. (2012). The mutational landscape of lethal castration-resistant prostate cancer. *Nature* **487**, 239–243.

[21] Roehl KA, Han M, Ramos CG, Antenor JA, and Catalona WJ (2004). Cancer progression and survival rates following anatomical radical retropubic prostatectomy in 3,478 consecutive patients: long-term results. *J Urol* **172**, 910–914.

[22] Han M, Partin AW, Piantadosi S, Epstein JI, and Walsh PC (2001). Era specific biochemical recurrence-free survival following radical prostatectomy for clinically localized prostate cancer. *J Urol* **166**, 416–419.

[23] Chun FK, Graefen M, Zacharias M, Haese A, Steuber T, Schlomm T, Walz J, Karakiewicz PI, and Huland H (2006). Anatomic radical retropubic prostatectomy—long-term recurrence-free survival rates for localized prostate cancer. *World J Urol* **24**, 273–280.

[24] Tsiatis AC, Norris-Kirby A, Rich RG, Hafez MJ, Gocke CD, Eshleman JR, and Murphy KM (2010). Comparison of Sanger sequencing, pyrosequencing, and melting curve analysis for the detection of KRAS mutations: diagnostic and clinical implications. *J Mol Diagn* **12**, 425–432.

[25] Setlur SR, Mertz KD, Hoshida Y, Demichelis F, Lupien M, Perner S, Sboner A, Pawitan Y, Andrén O, Johnson LA, et al. (2008). Estrogen-dependent signaling in a molecularly distinct subclass of aggressive prostate cancer. *J Natl Cancer Inst* **100**, 815–825.

[26] Khani FMJ Park K, et al. (2013). Evidence for molecular differences in prostate cancer between African American and Caucasian men. submitted for publication.

[27] Ralser M, Querfurth R, Warnatz HJ, Lehrach H, Yaspo ML, and Krobitsch S (2006). An efficient and economic enhancer mix for PCR. *Biochem Biophys Res Commun* **347**, 747–751.

[28] Gonzalez-Bosquet J, Calcei J, Wei JS, Garcia-Closas M, Sherman ME, Hewitt S, Vockley J, Lissowska J, Yang HP, Khan J, et al. (2011). Detection of somatic mutations by high-resolution DNA melting (HRM) analysis in multiple cancers. *PLoS One* **6**, e14522.

Supplementary Materials and Methods

Patient Population and Patient-Related Variable

Tumor staging and grading were standardized to the 2002 American Joint Committee on Cancer recommendations. After RP, patients were followed until death for disease recurrence. BCR was defined as a serum PSA level > 0.2 ng/ml on more than two consecutive occasions for the WCMC and AA cohorts. BCR in the Zurich cohort was defined as any increase in postoperative PSA > 0.1 ng/ml after achieving a PSA nadir < 0.1 ng/ml, while the Korean cohort defined BCR as any postoperative PSA > 0.2 ng/ml after achieving a PSA nadir < 0.1 ng/ml. Follow-up data on BCR was present in 537 patients (54.0%), and survival data were present on 226 patients (22.6%).

Swedish Watchful Waiting Cohort

The SWWC, as described previously [25], consisted of non–PSA-screened men with localized prostate cancer diagnosed by TURP and managed with watchful waiting. A subset of this population (141 patients) had FFPE specimens that were satisfactory for evaluation, of which 99 had DNA of sufficient quality and were included in this study. *SPOP* status was determined by performing HRM assay followed by Sanger sequencing. *ERG* rearrangement, *PTEN* deletions, and *CHD1* deletions were detected by FISH.

Korean Cohort

The Korean cohort consists of 127 consecutive patients with prostate cancer treated by robotic-assisted laparoscopic prostatectomy (RALP) at Kyungpook National University School of Medicine. The majority of these patients were found to have prostate cancer because of obstructive lower urinary tract symptoms; PSA is not routinely used as a screening tool in South Korea. Of the 127 patients, 87 had DNA of sufficient quality for evaluation. Slides of FFPE tissue from RALP were reviewed by study pathologists to confirm diagnosis and the pathologic characteristics, including Gleason grade, surgical margin, and pathologic stage. *SPOP* status was screened by performing HRM assay followed by Sanger sequencing. *ERG* status was annotated by immunohistochemistry and FISH. *PTEN* deletions were also identified by FISH.

USZ Cohort

FFPE prostate tissues from 421 consecutive men who underwent either RP (336), TURP (56), or metastasis (29) collection were obtained at the University Hospital of Zurich between 1993 and 2007 [12]. Slides of FFPE tissue were reviewed by study pathologists to confirm diagnosis and the pathologic characteristics, including Gleason grade, surgical margin, and pathologic stage. Of the 421 specimens, 251 were of sufficient quality to be analyzed. *SPOP* status was screened by performing HRM assay followed by Sanger sequencing. *ERG* rearrangements, *CHD1* deletions, and *PTEN* deletions were determined by performing FISH.

MSKCC Cohort

A total of 218 fresh frozen tumor samples were obtained from patients treated by RP at MSKCC, as previously described [13]. Eighty patients had DNA that could be reliably analyzed for this study. There were no significant differences in Gleason grade, stage, or clinical outcomes between the 80 cases from MSKCC that had evaluable DNA for SPOP and the 138 cases that did not have evaluable DNA. The percentage of tumor tissue *versus* normal tissue was at least 70% to be extracted [13]. *SPOP* status was identified by Sanger sequencing. *ERG* rearrangements were inferred using outlier mRNA expression, and *PTEN* and *CHD1* deletions were determined from array comparative genomic hybridization (CGH), as previously described [13].

WCMC Cohort

Tumors for the WCMC cohort were collected from 125 patients undergoing RALP from 2007 to 2010 by one single surgeon at a single institution. Cores in areas with high tumor density have been taken with an overall average of at least 60% tumor material. All African American patients were excluded from the WCMC cohort and grouped into a separate cohort. *SPOP* status was collected from previously reported whole exome data, RNA-Seq data, as well as Sanger sequencing [5]. We excluded four *SPOPmut* cases that showed inconsistent results between detection methods. *ERG* status was determined using FISH and immunohistochemistry (IHC); *CHD1* deletions and *PTEN* deletions were identified using FISH and CGH as previously described [5].

AA Cohort

Archival RP from 105 consecutive self-identified African American men were obtained at WCMC between 2001 and 2009, of which 88 had evaluable DNA. *SPOP* status was screened by performing HRM assay followed by Sanger sequencing. *ERG* expression was determined by IHC, and identification of *ERG* rearrangement and *PTEN* deletion was done by FISH. Molecular and clinical details of this cohort have been reported elsewhere [26].

Determining if SPOPmut *Prostate Cancer Is Associated with a Morphologic Phenotype*

A subset of 118 unselected prostate cancers from the WCMC was assessed. This group included 11 *SPOPmut* cases. Blinded to mutation status, two reviewers at WCMC assessed all prostatectomy slides from these 11 *SPOPmut* cancers and 11 *SPOPwt* cases with similar Gleason score and pathologic stage. Each prostatectomy specimen was assessed for the presence or absence of 15 morphologic features of prostate cancer: intraductal spread, cribriform morphology, blue-tinged mucin, crystalloids, high nucleocytoplasmic ratio, macronucleoli, foamy gland features, collagenous micronodules, small cell/neuroendocrine differentiation, perineural invasion, extraprostatic extension, signet ring–like cell features, ductal morphology, glomerulations, and comedonecrosis. Statistical analysis was performed to look for significant associations between morphology and *SPOPmut* status.

DNA Extraction

Citrosolve (400 µl) was added to each well of a 96-well plate. The plate was then placed on a shaking pad, followed by incubation on a heat plate for 10 minutes, placed back on the shaking pad, and repeated for a total of three times. After the three cycles, the citrosolve was removed and the samples received two 400 µl of ethanol washes. After a 1-hour drying step, 300 µl of AL tissue lysis buffer was added in addition to 20 µl of proteinase K solution for an overnight incubation. Two additional sets of 20 µl of proteinase K were added if cores were still visible, and each time incubated at 55°C for 3 hours with intervals of shaking. After digestion, 300 µl of lysis buffer and 600 µl of ethanol were added to the lysate and the samples were transferred to a filter column. AW1 and AW2 wash buffers with two doses of 96% ethanol were added

to purify the samples. DNA was then eluted in two steps in 50 µl of AE buffer by centrifugation. DNA was quantified using the Nanodrop spectrophotometer. Samples with a DNA concentration of 20 to 50 ng/µl or above were included in the study. DNA purity was determined by measuring UV absorbance [15]. DNA extraction from the WCMC cohort [5] and MSKCC cohort [15] has been previously described. DNA from patients of the hospital of Zurich was extracted by using the blood and tissue kit (Qiagen) as suggested by the manufacturer.

Targeted Enrichment for SPOP *Exons 6 and 7*

The pre-PCR reactions were performed in 30-µl volumes. For the exon 6 assay, 1 µl of patient DNA (30-80 ng), 2 µl of working primer solution (forward + reverse, 3 µM concentration), 2.4 µl of 50 mM $MgCl_2$, 4 µl of 10 mM deoxyribonucleotide (dNTP) solution (Invitrogen, Carlsbad, CA), 2 µl of 1.5 mM High-Fidelity PCR Buffer (Thermo Scientific, Waltham, MA), and 17.8 µl of sterile water were used. For the exon 7 assay, the process was the same as for exon 6 except for the addition of 11.8 µl of sterile water and 6 µl of 5× combinatorial enhancer solution (CES) enhancer solution [27].

Pre-PCR was performed on Eppendorf Mastercycler Pro. Optimized cycling conditions used for both assays are given as follows: initial activation step at 98°C for 1 minute, followed by 30 cycles of 95°C for 5 seconds, 60°C for 10 seconds, and 72°C for 30 seconds. After a final step of 72°C for 30 seconds, samples were held at 4°C. (For complete list of primers, see Table W1.)

HRM Analysis

Pre-PCR products were diluted 1:100 with sterile water. Samples were run in triplicate on the LightCycler 480 II (Roche Diagnostics, Basel, Switzerland). A total reaction volume of 10 µl was used, which consisted of 1 µl of diluted pre-PCR products and 3 µM forward and reverse HRM primers, 5 µl of High Resolution Melting Master Mix (from Roche), 1 µl (exon 6 assay) or 1.4 µl (exon 7 assay) of 25 mM $MgCl_2$ plus 2 µl (exon 6 assay) or 1.6 µl (exon 7 assay) of PCR-grade water.

HRM conditions used were given as follows: An activation step of 10 minutes at 95°C is followed by 30 cycles of 10 seconds at 55°C and 72°C for 30 seconds. Before the HRM, a heteroduplex forming step that involves heating the PCR products to 95°C for 1 minute and a rapid cooling to 45°C for 1 minute is performed. HRM was performed from 72°C to 95°C at a temperature gradient of 1°C per second, acquiring 30 data points per °C. (For complete list of primers, see Table W1). This assay targets two exons of the *SPOP* gene containing all previously detected mutations in prostate cancer (amino acids 80 to 106 and amino acids 120 to 140).

The melting curves were normalized at the pre-melt (100% fluorescence) and post-melt (0% fluorescence) stages using gene scanning software (Roche) [28]. Further assay details and cycling conditions can be found in the Supplementary Materials and Methods. Seven controls were run in each assay along with 96 samples on a 384-well plate. Normalization of the melting curves was done using these controls. The controls used were five known heterozygous mutations F133V, F133C, K129E, F102C, and Y87C and two known wild-type controls (one for exon 6 and one for exon 7). The average size of 50 to 150 bp of the targeted fragment is notable, as the use of archival material, such as DNA from FFPE material, can show a high degree of degradation. Every sample that showed a notable shift in the melting curve was sent off for Sanger sequencing to confirm and further specify its alteration.

To determine the assay sensitivity, plasmid DNA of mutated SPOP was mixed with plasmid DNA of wild-type SPOP in different ratios. This allows us to investigate the sensitivity in the most accurate manner and leads to the highest possible sensitivity under best conditions.

DNA Capture, Library Preparations, and MiSeq Runs

By using the Illumina DesignStudio application (http://www.illumina.com/applications/designstudio.ilmn), we designed a customized TrueSeq amplicon kit to cover all exons of *SPOP* (~3.5 kb). Forty-six amplicons with an average size of 174nt (±6) were designed. All samples were run on one lane of MiSeq that generated 13 Mb paired end reads (2 × 250 bp) for a total of ~6.5 Gb.

The library preparation was performed as suggested by the manufacturer (http://supportres.illumina.com/documents/myillumina/b718c350-b3b2-4234-b71a-0b832f14cda3/truseq_custom_amplicon_libraryprep_ug_15027983_b.pdf). We considered samples passing quality control (QC) if they had more than 250 ng in 5 µl, quantified by Qubit, and a minimal fragment size of 45 bp, determined by Bioanalyzer.

Table W1. Sequence of Primers.

SPOP Gene	Primer Name	Sequence (5′-3′)	Amplicon Size (bp)
Pre-PCR			
Exon 7	SPOP_E7_PPCR_R	AGT TGT GGC TTT GAT CTG GTT	240
Exon 7	SPOP_E7_PPCR_F	ACT CAT CAG ATC TGG GAA CTG C	
Exon 6	SPOP_E6_PPCR_F	ACC CAT AGC TTT GGT TTC TTC TCC C	170
Exon 6	SPOP_E6_PPCR_R	TAT CTG TTT TGG ACA GGT GTT TGC G	
HRM			
Exon 7	SPOP_E7_HRM_R	TTT CCC ACC CCA GAG AGT	102
Exon 7	SPOP_E7_HRM_F	GTT GGC CTC ATC CAA AAG AA	
Exon 6	SPOP_E6_HRM_F	TCT TCT CCC TTG GCA TTC AG	123
Exon 6	SPOP_E6_HRM_R	CCC CAA AGG GTT AGA TGA AGA	
Sequencing			
Exon 7	SPOP_E7_PPCR_F	ACT CAT CAG ATC TGG GAA CTG C	
Exon 6	SPOP_E6_PPCR_R	TAT CTG TTT TGG ACA GGT GTT TGC G	

The sequence of primers was used for the pre-PCR, HRM, as well as Sanger sequencing.

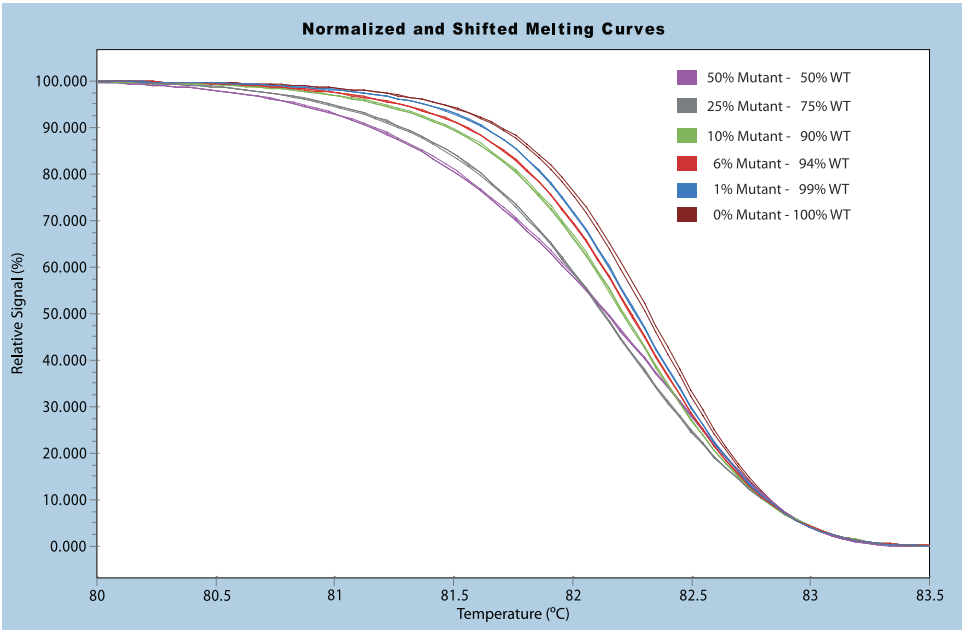

Figure W1. Sensitivity of HRM. The HRM curves for a serial dilution of mutated and wild-type DNA are shown. The purple melting curve consists of 50% mutant and 50% wild-type DNA, gray of 25% mutant and 75% wild-type, green of 10% mutant and 90% wild-type DNA, red of 60% mutant and 40% wild-type DNA, blue of 1% mutant and 99% wild-type DNA, and brown of 100% wild-type DNA.